Roles of a conserved proline in the internal fusion peptide of Ebola glycoprotein

María J. Gómara[a], Puig Mora[b], Ismael Mingarro[b], José L. Nieva[a,*]

[a] *Unidad de Biofísica (CSIC-UPV/EHU) y Departamento de Bioquímica, Universidad del País Vasco, Aptdo. 644, 48080 Bilbao, Spain*
[b] *Departament de Bioquímica i Biologia Molecular, Universitat de València, E-46100 Burjassot, València, Spain*

Received 3 March 2004; revised 21 May 2004; accepted 3 June 2004

Available online 15 June 2004

Edited by Hans-Dieter Klenk

Abstract The structural determinants underlying the functionality of viral internal fusion peptides (IFPs) are not well understood. We have compared EBO_{wt} (GAAIGLAWIPYFGPAAE), representing the IFP of the Ebola fusion protein GP, and EBO_{mut} (GAAIGLAWIPYFGRAAE) derived from a non-functional mutant with conserved Pro537 substituted by Arg. P537R substitution did not abrogate peptide-membrane association, but interfered with the ability to induce bilayer destabilization. Structural determinations suggest that Pro537 is required to preserve a membrane-perturbing local conformation in apolar environments.

Keywords: Ebola glycoprotein; Viral fusion peptide; Peptide–lipid interaction; Peptide conformation; Protein insertion into membranes; Proline

1. Introduction

It is currently postulated that viral proteins mediating virus-cell fusion processes insert into target cell membranes through specialized hydrophobic sequences termed "fusion peptides" (FPs) [1–3]. These conserved domains are absolutely required for the fusogenic activity, but the structural and functional determinants that constrain their amino acid compositions remain unknown. While several FPs are free N-terminal sequences of the polypeptide chain that protrude from the surface of the virion, others constitute internal sequences [2,4]. An important body of experimental information is available on the way N-terminal fusion peptides (NFPs) become integral in membranes, as well as on the type of perturbations they may induce therein [for reviews see [5–7]]. Comparatively less is known on the type of interactions established by internal fusion peptides (IFPs) with membranes.

Predictive structural analyses indicate that IFPs are segmented into two regions intervened by a putative turn or a loop, which usually contains one or more Pro residues [8]. This organization seems to be fundamental to sustain the fusogenic function [8]. Gallaher [4] predicted the existence of an IFP in GP2, the fusogenic subunit of Ebola surface protein GP [9,10]. Biophysical characterization by our group confirmed the ability of the predicted Ebola IFP sequence to associate with phosphatidylinositol (PI)-containing lipid vesicles and perturb their integrity [11,12]. Mutational analysis by Ito et al. [13] further supported a fusion peptide role for this GP2 sequence. These authors showed that non-conservative substitutions of Pro residues in positions 533 and 537 impair GP functionality. In particular, P533R substitution renders an Ebola GP2 protein deficient in maturation, while P537R abolishes GP2 activity without affecting transport to cell surface or incorporation into virions. This suggests that the conserved Pro537 is directly involved in the Ebola-cell fusion process mediated by GP2.

In order to establish the specificity of Ebola IFP-induced membrane destabilization and the involvement of the conserved Pro537 in the process, we compare here EBO_{wt} (GAAIGLAWIPYFG**P**AAE) and EBO_{mut} (GAAIGLAWIPYFG**R**AAE), two synthetic sequences that represent IFP domains (residues 524–540) in fusion-active and fusion-inactive GP2 proteins, respectively. Our data support the notion that Pro and Arg residues at position 537 promote the adoption of different structures in the low-polarity membrane environment. The P537R substitution confers to the sequence an affinity for electrically neutral phosphatidylcholine (PC) membranes, but abrogates the ability to destabilize large unilamellar vesicles (LUV) composed of anionic PI. Tyr-to-Trp energy transfer and circular dichroism suggest that Pro537 might be implied in stabilizing a turn-like structure, which would be maintained in the membrane apolar milieu. We conclude that IFP insertion into the target membrane is not enough to sustain Ebola GP activity, and propose that adoption of an interfacial Pro-based structure is crucial for the promotion of membrane destabilization during Ebola virus-cell fusion.

2. Materials and methods

1-Palmitoyl-2-oleoylphosphatidylcholine (POPC), liver PI, *N*-(7-nitro-benz-2-oxa-1,3-diazol-4-yl)phosphatidylethanolamine (N-NBD-PE) and *N*-(lissamine Rhodamine B sulfonyl)phosphatidylethanolamine

* Corresponding author. Fax: +34-94-6013360.
E-mail address: gbpniesj@lg.ehu.es (J.L. Nieva).

Abbreviations: ANTS, 8-aminonaphthalene-1,3,6-trisulfonic acid sodium salt; CD, circular dichroism; DPX, *p*-xylenebis(pyridinium)bromide; EBO_{wt}, synthetic GAAIGLAWIPYFGPAAE amino acid sequence; EBO_{mut}, synthetic GAAIGLAWIPYFGRAAE amino acid sequence; IFP, internal fusion peptide; LUV, large unilamellar vesicles; NATA, *N*-acetyl-L-tryptophanamide; NFP, N-terminal fusion peptide; POPC, 1-palmitoyl-2-oleoylphosphatidylcholine; PI, phosphatidylinositol; RET, resonance energy transfer; TFE, trifluoroethanol

0014-5793/$22.00
doi:10.1016/j.febslet.2004.06.006

(N-Rho-PE) were purchased from Avanti Polar Lipids (Birmingham, AL, USA). 8-Aminonaphthalene-1,3,6-trisulfonic acid sodium salt (ANTS) and *p*-xylenebis(pyridinium)bromide (DPX) were from Molecular Probes (Junction City, OR, USA). D_2O, trifluoroethanol (TFE), *N*-acetyl-L-tryptophanamide (NATA) and Triton X-100 were obtained from Sigma (St. Louis, MO, USA). All other reagents were of analytical grade. The GAAIGLAWIPYFGPAAE (EBO_{wt}) and GAAIGLAWIPYFGRAAE (EBO_{mut}) peptides were synthesized by solid-phase synthesis using Fmoc chemistry as C-terminal carboxamides and purified (estimated homogeneity >90%) by HPLC. Peptide stock solutions were prepared in dimethyl sulfoxide (spectroscopy grade). The YW, PY and AW dipeptides used for calibrating energy transfer experiments were obtained from Bachem (Bubendorf, Switzerland).

LUV were prepared following the extrusion method of Hope et al. [14] in 5 mM HEPES and 100 mM NaCl (pH 7.4) buffer. Release of vesicular contents to the medium and mixing of lipids were monitored by the ANTS/DPX and resonance energy transfer (RET) assays, respectively, as described in [15]. Trp-fluorescence emission of peptides in the presence of LUV was recorded in a Perkin–Elmer MPF-66 spectrofluorimeter with excitation set at 280 nm. The signal was further corrected for dilution and inner filter effects using the soluble Trp analog NATA following the procedure described in [16]. Tyr to Trp energy transfer in EBO_{wt} and EBO_{mut} was measured according to the methods described in [17,18]. Peptide excitation spectra (emission set at 345 nm, at which only Trp emits) were compared with spectra obtained for transfer efficiencies (e) of 1 and 0. The $e = 1$ and $e = 0$ references were experimentally obtained using YW (1 μM), and an equimolar mixture of PY and AW (1 μM each), respectively. Subtraction from YW excitation spectrum (normalized to the intensity value at $\lambda = 295$ nm) yields the "excitation difference spectrum" for each peptide. Efficiency of transfer from Tyr to Trp (e_{tyr}) was calculated by adjusting the excitation difference spectrum to:

$$Q(\lambda) = f_{trp}(\lambda) + e_{tyr} f_{tyr}(\lambda) \quad (1)$$

where $Q(\lambda)$ is the relative quantum yield of Trps excited at wavelength λ, and f_{trp} and f_{tyr} are the fractions of light absorbed by Tyr and Trp as obtained from absorption spectra using PY-AW mixtures.

Circular dichroism (CD) measurements were carried out on a thermally controlled Jasco 810 CD spectropolarimeter (Eaton, USA) calibrated routinely with (1*S*)-(+)-10-camphorsulfonic acid and ammonium salt. The spectra were measured in a 1 mm path-length quartz cell. Data were taken with a 0.1 nm step size, 50 nm/min speed, and the results of 10 scans were averaged. CD spectra were taken at 25 °C in 5 mM HEPES, 100 mM NaCl (pH 7.4). Peptide concentration was 30 μM as determined by UV spectroscopy using $\varepsilon = 1450\ M^{-1}cm^{-1}$ for tyrosine and $\varepsilon = 5570\ M^{-1}cm^{-1}$ for tryptophan [19]. To simplify the comparison between different TFE percentages and to verify the average secondary structure content, ellipticity spectra were converted from millidegrees to secondary structure fractions using model-protein CD spectra [20], according to the software specifications (Jasco Secondary Structure Estimation Version 1.00).

3. Results and discussion

According to the current model of viral fusion, FPs bear an intrinsic capacity to disrupt the target bilayer architecture after insertion and directly mediate membrane merging [1–7]. Sequence features listed below suggest that Ebola IFP might adopt a bent structure at membrane interfaces. First, plot in Fig. 1A shows the tendency to adopt interfacial turns within Ebola IFP sequence. Specifically, the dominance of turn-inducing residues (normalized turn potential >1) over non-inducing ones (turn potential <1) is clearly noticeable in the inter-Pro region, in which virtually all residues are turn inducers. This suggests that within Gly- and Ala-rich Ebola IFP sequence, Pro residues might structurally constrain the inherently flexible sequence into a bent conformation. Sequence alignment (Fig. 1B) further reveals that the inter-Pro region is absolutely conserved among Ebola strains, while in Marburg this region displays a conservative Phe × Tyr substitution.

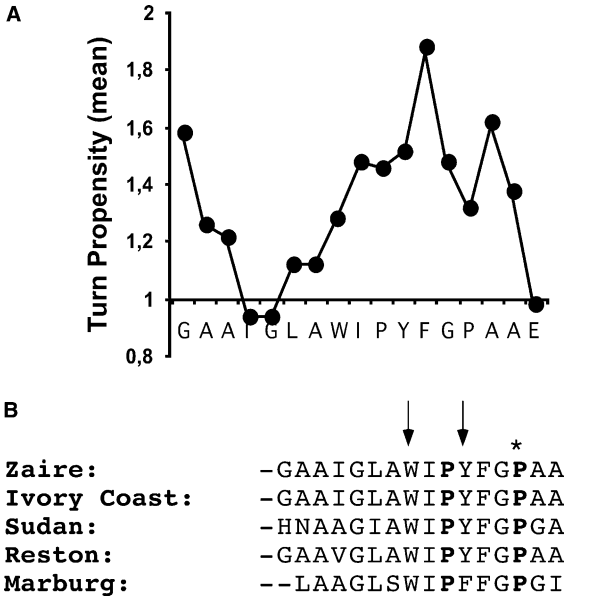

Fig. 1. (A) Turn propensity within Ebola IFP. Normalized turn potentials described by Monné et al. [31] for model transmembrane sequences were used to calculate average values within sliding windows of five amino acids. (B) Multiple sequence alignment of filovirus IFP domains by CLUSTALW. Invariant Pro residues are indicated in bold. Pro537 is denoted by "*", and Trp531 and Tyr534 (positions in Zaire strain) are denoted by arrows.

Second, Ebola IFP would minimize its interacting energy by remaining associated with the membrane interface region (Table 1). The calculated free energies of transfer from water to membrane interfaces computed for the unfolded (ΔG_{wiu}) and folded (ΔG_{wif}) Ebola IFP sequences are clearly larger than ΔG_{wo}, which corresponds to the free energy of inserting

Table 1
Energetics of FP-membrane partitioning in processed type I viral fusion proteins

	FP type	ΔG_{wiu}[a]	ΔG_{wif}[a]	ΔG_{wo}[a]
Ebola GP[b]: (524–539)	IFP	−3.3	−11.3	−1.8
HIV-1 *env*: (512–527)	NFP	−3.4	−11.4	−1.0
Influenza HA[c]: (340–355)	NFP	−0.4/−4.5	−7.6/−12.5	5.9/−1.2
Sendai F: (117–132)	NFP	−2.3	−10.3	−1.9
RSV *env*: (427–442)	IFP	−0.6	−8.6	−1.4

Free energies (ΔG) are given in kcal mol^{-1}.
[a] wiu, transfer from water to interface, unfolded; wif, transfer from water to interface, folded; wo, transfer from water to octanol [21,22].
[b] Computed for 16 residues, comprising N-termini of NFPs, and homologous most hydrophobic stretches of IFPs. Gene Bank accession numbers: U31033 (Ebola GP); M15654 (HIV-1 *env*); M31689 (Influenza HA); M12396 (Sendai F); V01197 (RSV *env*).
[c] Computed for unprotonated/protonated Asp and Glu residues.

α-helical amino acid residues into the bilayer hydrophobic core [21,22]. Thus, energy values in Table 1 are consistent with a preference of Ebola IFP for remaining associated to the membrane interface region (rather than for adopting transmembrane configurations) when the sequence is transferred from water into membranes, as proposed to occur during the fusion reaction cycle [1–7]. In general, values listed in Table 1 show similar trends among NFPs and IFPs derived from class I fusion proteins that activate upon cleavage [2].

The previous analyses suggest a functional role for the Ebola IFP inter-Pro region. Therefore, we explored in experimental model systems the effects of P537R substitution, described to abolish Ebola GP function. Direct implication of FPs in virus-cell fusion is supported by studies using model membranes, membrane mimetic systems and synthetic peptide fragments representing functional and non-functional FP sequences, which demonstrate that, after insertion, only functional sequences generate target-membrane perturbations (reviewed in [7]). The initial perturbations seem to originate at their capacity to form pores, an effect that may result in the permeabilization of dispersed vesicles. Thus, induction of vesicle permeability has been shown to correlate well with FP functionality in most instances. In principle, P537R substitution might affect IFP capacity to insert into membranes, or interfere with the adoption of a functional destabilizing structure. Fig. 2 illustrates the effect of this mutation on the ability of the peptide to associate with and destabilize phospholipid vesicles. Addition of EBO_{wt} to PI LUV at high peptide-to-lipid mole ratios induced vesicle destabilization and leaking out of aqueous contents (panels A and B). In accordance with previously reported results showing the incapacity of this peptide to associate with PC-based vesicles [11], the wt peptide did not destabilize POPC LUV. The P537R-representing EBO_{mut} was unable to induce contents efflux from PI or POPC vesicles even at the highest peptide-to-lipid mole ratio tested. However, changes in fluorescence emission of the single Trp in the presence of LUV confirmed that EBO_{mut} was indeed able to interact with PI, as well as with POPC vesicles (panel C). The emission in buffer of EBO_{mut}, 355 nm, shifted to lower wavelengths upon addition of LUV or in the presence of membrane-mimic TFE (25% v/v), while the fluorescence intensity increased. These changes reflect that the tryptophan residue, fully exposed to water in buffer, moves to an environment of lower polarity provided by the vesicles or the organic solvent [18]. In comparison EBO_{wt}-Trp emission was centered at 347 nm in buffer and did not significantly change in presence of LUV or after TFE (25% v/v) addition. This observation suggests that EBO_{wt}-Trp in membranes is partially shielded from water but remains in contact with hydrogen-bonding groups [18], which is consistent with immersion of the fluorophore into the membrane-water interface environment.

In summary, P537R-representing IFP sequence is deficient at inducing membrane perturbations upon membrane insertion, a fact that correlates well with the blocking effect exerted by this mutation on Ebola GP activity. Moreover, P537R-like substitution enables insertion into POPC bilayers. A possible explanation for this effect might be that, in contrast to the parental sequence, the Arg-containing variant undergoes partitioning-coupled folding in this model system. In support of this notion, it should be mentioned that Arg side chain is largely hydrophobic, with the charged moiety at the tip, and, therefore, able to reach up into the water-membrane interface,

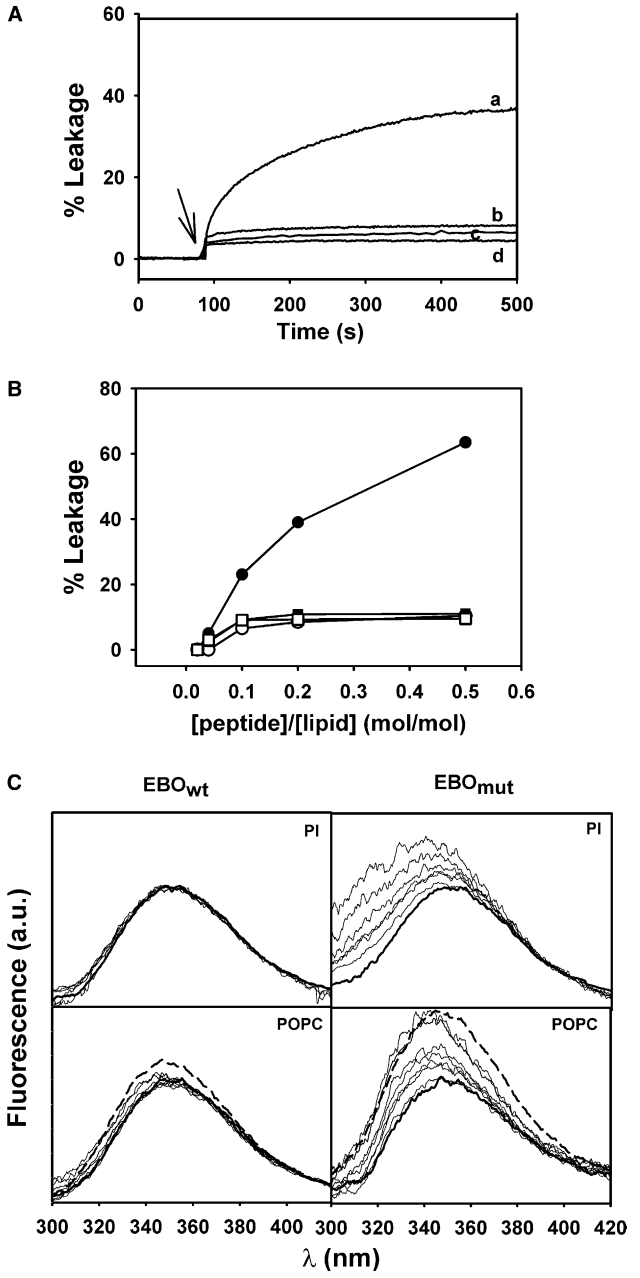

Fig. 2. Interaction of EBO_{wt} and EBO_{mut} with lipid vesicles. (A) Peptide-induced LUV permeabilization (ANTS/DPX efflux) as a function of time (peptides added at the time indicated by the arrow); a: EBO_{wt} and PI LUV, b: EBO_{wt} and POPC LUV, c: EBO_{mut} and PI LUV, and d: EBO_{mut} and POPC LUV. In all cases, lipid concentration was 50 μM and the added peptide-to-lipid mole ratio, 0.2. (B) Permeabilization of PI (circles) and POPC (squares) vesicles induced by EBO_{wt} (filled symbols) and EBO_{mut} (empty symbols) as a function of the added peptide-to-lipid mole ratio. Final extents were measured 10 minutes after peptide addition. Conditions otherwise as in (A). (C) Fluorescence emission spectra of EBO_{wt} and EBO_{mut} incubated with increasing amounts of POPC or PI LUV. Lipid concentrations were (spectra from right to left): 0 (absence of lipid, thick line), 25, 75, 100, 250, 500 and 750 μM. Peptide concentration was 1 μM. Thick dashed lines in bottom panels correspond to the emission spectra in the presence of TFE (25% v/v).

even from positions located quite deep into the hydrophobic core of the bilayer [23]. We postulate that PI bilayer sustains interactions of wild-type Ebola IFP because its interface, rich

in H-bonding moieties, provides the suitable environment for inserting a partially folded inter-Pro bent rigid structure. Thus, our hypothesis states that inter-Pro region would not undergo major conformational changes in low-polarity environments, whereas, in the absence of the conformational constraints imposed by Pro537, it would transit to a different local structure.

To test the former hypothesis, we first measured the energy transfer between donor Tyr534, located within the inter-Pro region (Fig. 1), and acceptor Trp531, in environments of different polarity. Tyr-to-Trp energy transfer efficiency ("*e*", dotted lines in Fig. 3) was calibrated in the different media considering the relative absorbance of the aromatic residues in mixtures of Ala-Trp and Pro-Tyr dipeptides [17,18]. The Tyr-to-Trp "*e*" values within EBO_{wt} and EBO_{mut} sequences were experimentally obtained by measuring the Trp-emission (set at 345 nm) for various excitation wavelengths. Under the same experimental conditions, Trp–Tyr dipeptide emission was considered to correspond to $e = 1$. The trp excitation difference spectra (solid and dashed lines in Fig. 3) were computed relative to Trp-Tyr excitation spectrum, which was normalized to the value obtained at excitation of 295 nm, where only Trp absorbs. Trp excitation difference spectra are shown for the peptides in buffer (panel A) and in the presence of TFE (25% v/v) (panel B). Comparable efficiencies ($e \approx 0.2$) were measured in buffer for both peptides. After peptide structuring in the presence of TFE, transfer efficiency in EBO_{mut} significantly

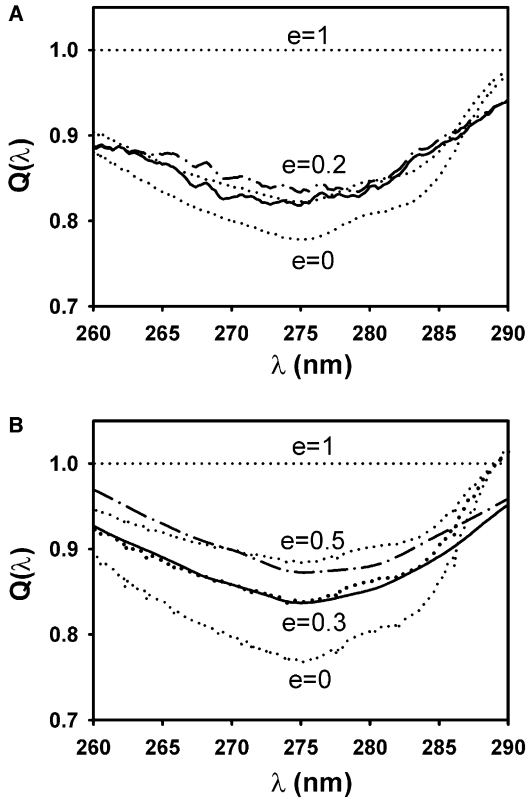

Fig. 3. Wavelength dependence of the relative quantum yield of Trp in buffer (panel A) and in the presence of TFE (25% v/v) (panel B). The dotted curves correspond to spectra based on the fractional absorbances. Energy transfer efficiency values (*e*) were calculated according to Eq. (1). Relative quantum yields of Trp531 are denoted by solid (EBO_{wt}) and dashed spectra (EBO_{mut}).

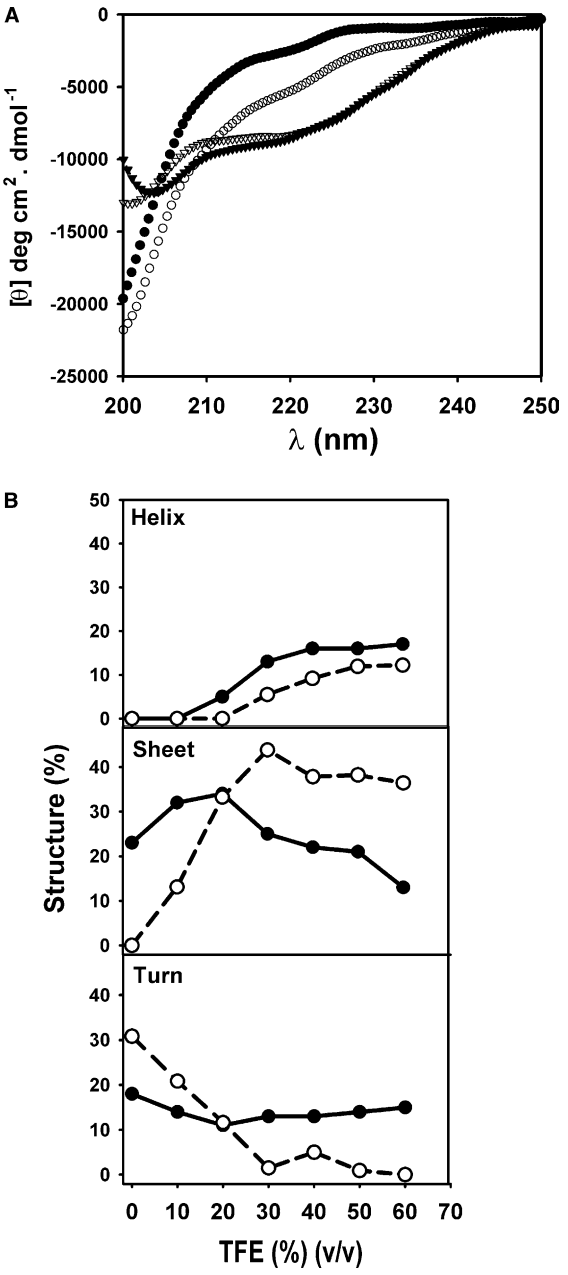

Fig. 4. Structural CD determination. (A) Far UV CD spectra in buffer (circles) and in the presence of TFE (25% v/v) (inverted triangles) of EBO_{wt} (filled symbols) and EBO_{mut} (empty symbols). Spectra values are expressed as mean molar ellipticity per residue. Peptide concentration was 30 μM. (B) Structure content of EBO_{wt} (filled symbols and solid line) and EBO_{mut} (empty symbols and dashed line) as a function of the TFE concentration. Conditions otherwise as in panel (A).

increased ($e \approx 0.5$) while that measured in EBO_{wt} remained roughly the same ($e \approx 0.3$). These data indicate that the intramolecular Tyr-to-Trp distance in EBO_{wt} is not appreciably affected by low-polarity, while it changes by becoming shorter in EBO_{mut}.

CD spectra measured in environments of decreasing polarity also confirmed the existence of conformational differences between EBO_{wt} and EBO_{mut} peptides (Fig. 4). Spectra in buffer (Fig. 4A) indicated mainly random conformations for both peptides. However, ellipticities measured at 220 nm were

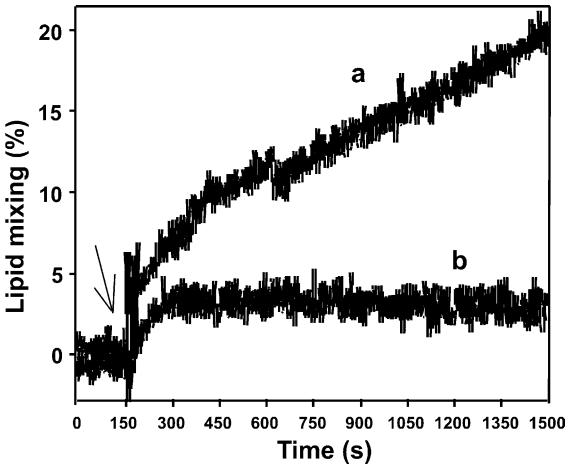

Fig. 5. Calcium-assisted fusion (membrane lipid mixing, RET assay) of PI LUV. Mixing of lipids as a function of time after addition (indicated by the arrow) of EBO_{wt} (a) or EBO_{mut} (b). The peptides were added at the peptide-to-lipid mole ratio of 0.2 and final calcium concentration was 5 mM. Lipid concentration was 100 μM.

consistent with the EBO_{wt} sequence becoming more structured than EBO_{mut} in low-polarity solvents. In the case of EBO_{wt}, increasing amounts of TFE induced stabilization of α-helical structures, which seemed to be produced at the expense of the initial β-type structure content, while the turn content remained roughly constant at all studied TFE concentrations (Fig. 4B). In contrast, TFE contributed to stabilize α-helical and β-type structures in EBO_{mut}, while turns were virtually eliminated in the low-polarity medium. Thus, CD determinations would be consistent with the presence in Ebola IFP of turn-like structures in aqueous buffer that are preserved in low-polarity environments. The fact that P537R substitution caused the loss of such component in the low-polar medium supports the involvement of Pro537 in sustaining this type of conformations.

Finally we tested the effect of P537R substitution in the context of fusion assisted by calcium [7,12]. So far, our results indicate that the sequence derived from the wild-type Ebola IFP is capable to induce perturbations in dispersed vesicles. This process mimics initial interactions of GP ectodomain with target bilayer. Formation of helical bundles after GP activation is postulated to bring into close contact the membranes to be fused [24,25]. Subsequent membrane merger evolves within apposed bilayers through a defined pathway of lipidic intermediates [2,5,7]. In order to test the activity of FP sequences in aggregated bilayers, in previous works we have used cations to modulate the aggregational state of membranes [12,15]. Particularly, EBO_{wt} has been shown to induce fusion (membrane lipid-mixing) of PI LUV in the presence of 5 mM Ca^{2+} [12]. Results displayed in Fig. 5 demonstrate that EBO_{mut} was deficient at inducing lipid-mixing under similar experimental conditions.

4. Concluding remarks

Ebola GP2 belongs to class I of viral fusion proteins [26]. The model for GP2-mediated fusion postulates that formation by the ectodomain of a low-energy helical bundle facilitates close apposition of viral and cell membranes, which would be anchored through transmembrane and IFP domains, respectively [24,25]. Within this framework, the results in this work support an active role for viral IFPs in membrane destabilization during the fusion process. A single P537R substitution abolishes the capacity of the Ebola IFP sequence to induce aqueous content leakage from vesicles, but not its ability to associate with lipid bilayers. In addition, adoption of the initial perturbing structure might condition the ability of the sequence to catalyze subsequent steps along the fusion pathway. This argues against a passive role of the sequence as a featureless hydrophobic membrane anchor that inserts into the target cell membrane.

The fact that becoming integral to membranes does not by itself sustain FP functionality has also been confirmed for substitutions at the N-terminal region of HIV and influenza NFPs [7]. Similarly to the mutation described here, these substitutions do not impair NFP-membrane association but abolish NFP ability to destabilize lipid vesicles after insertion. The atomic structure of influenza fusion domain resolved in a micellar environment at pH 5.0 reveals the putative functional organization of NFPs [27]. The α-helical amino terminus is followed by a bent sequence that confers an inverted 'V' appearance to the structure. Recent structural studies indicate that G1V substitution, known to block hemagglutinin-induced fusion, might also alter the membrane-perturbing "inverted V" conformation adopted by influenza NFP in lipidic environments [28]. G1V mutation locks influenza NFP into a linear helical structure, which would be oriented approximately parallel to the membrane surface.

Our data support a role for Pro537 in sustaining a membrane-perturbing structure of Ebola IFP. Pro residues have been described to play important structural roles in membrane-inserted peptide chains, specifically promoting kinks at the level of the membrane interface (see [29] and references therein). In fact, it has been shown that Pro residues display the highest turn induction propensity at the membrane interface in poly(Leu) stretches [30,31]. We hypothesize that the presence of a bent located at the inter-Pro region of the Ebola IFP is directly related to its capacity to perturb membrane architecture. We also suggest that P537R substitution might unleash the interfacial bent structure and allow the adoption of a more linear state, which would be unable to promote the bilayer destabilization required for fusion development. High resolution NMR studies are under way with the aim of obtaining further support for these hypotheses.

Acknowledgements: This work was supported by MCyT (EET 2001/1954, BMC 2003-01532), the University of the Basque Country (UPV-42.310-13552) and the University of Valencia (UV-AE-20030395).

References

[1] Gallaher, W.R. (1987) Cell 50, 327–32887.
[2] White, J. (1990) Annu. Rev. Physiol. 52, 675–697.
[3] Skehel, J.J. and Wiley, D.C. (2000) Annu. Rev. Biochem. 69, 531–569.
[4] Gallaher, W.R. (1996) Cell 85, 477–478.
[5] Durell, S.R., Martin, I., Ruysschaert, J., Shai, Y. and Blumenthal, R. (1997) Mol. Membr. Biol. 14, 97–112.
[6] Han, X. and Tamm, L.K. (2000) Biosci. Rep. 20, 501–518.
[7] Nieva, J.L. and Agirre, A. (2003) Biochim. Biophys. Acta 1614, 104–115.

[8] Delos, S.E., Gilbert, J.M. and White, J.M. (2000) J. Virol. 74, 1686–1693.
[9] Volchkov, V.E. (1999) Curr. Top. Microbiol. Immunol. 235, 35–47.
[10] Feldmann, H., Volchkov, V.E., Volchkova, V.A. and Klenk, H.D. (1999) in: 100 Years of Virology (Calisher, C.H. and Horzinek, M.C., Eds.), pp. 159–169, Springer, Wien.
[11] Ruiz-Argüello, M.B., Goñi, F.M., Pereira, F.B. and Nieva, J.L. (1998) J. Virol. 72, 1775–1781.
[12] Suárez, T., Gómara, M.J., Goñi, F.M., Mingarro, I., Muga, A., Pérez-Payá, E. and Nieva, J.L. (2003) FEBS Lett. 535, 23–28.
[13] Ito, H., Watanabe, S., Sánchez, A., Whitt, M.A. and Kawaoka, Y. (1999) J. Virol. 73, 8907–8912.
[14] Hope, M.J., Bally, M.B., Webb, G. and Cullis, P.R. (1985) Biochim. Biophys. Acta 812, 55–65.
[15] Nieva, J.L., Nir, S., Muga, A., Goñi, F.M. and Wilschut, J. (1994) Biochemistry 33, 3201–3209.
[16] White, S., Wimley, W.C., Ladokhin, A.S. and Hristova, K. (1998) Methods Enzymol. 295, 62–87.
[17] Eisenger, J. (1969) Biochemistry 8, 3902–3908.
[18] Lakowicz, J.R. (1999) Principles of Fluorescence Spectroscopy, second ed. Academic/Plenum Publishers, New York.
[19] Pérez-Payá, E., Houghten, R.A. and Blondelle, S.E. (1996) J. Biol. Chem. 271, 4120–4126.
[20] Yang, J.T., Wu, C.S. and Martinez, H.M. (1986) Methods Enzymol. 130, 208–269.
[21] Wimley, W.C. and White, S.H. (1996) Nat. Struct. Biol. 3, 842–848.
[22] White, S.H., Ladokhin, A.S., Jayasinghe, S. and Hristova, K. (2001) J. Biol. Chem. 276, 32395–32398.
[23] Killian, A. and von Heijne, G. (2000) Trends Biochem. Sci. 25, 429–434.
[24] Weissenhorn, W., Carfi, A., Lee, K., Skehel, J.J. and Wiley, D.C. (1998) Mol. Cell. 2, 605–616.
[25] Malashkevich, V.N., Schneider, B.J., McNally, M.N., Milhollen, M.A., Pang, J.X. and Kim, P.S. (1999) Proc. Natl. Acad. Sci. USA 96, 2662–2667.
[26] Basañez, G. (2002) Cell. Mol. Life Sci. 59, 1478–1490.
[27] Han, X., Bushweller, J.H., Cafiso, D.S. and Tamm, L.K. (2001) Nat. Struct. Biol. 8, 715–720.
[28] Tamm, L.K. (2003) Biochim. Biophys. Acta 1614, 14–23.
[29] Orzáez, M., Salgado, J., Giménez-Giner, A., Pérez-Payá, E. and Mingarro, I. (2004) J. Mol. Biol. 335, 631–640.
[30] Monné, G., Hermansson, M. and von Heijne, G. (1999) J. Mol. Biol. 288, 141–145.
[31] Monné, G., Nilsson, I., Elofsson, A. and von Heijne, G. (1999) J. Mol. Biol. 293, 807–814.